



# Nanosized Magnesium Electrochemically Deposited on a Carbon Nanotubes Suspension: Synthesis and Hydrogen Storage

Chaoqi Shen and Kondo-Francois Aguey-Zinsou\*

MERLin, School of Chemical Engineering, The University of New South Wales, Sydney, NSW, Australia

## OPEN ACCESS

### Edited by:

Mariusz Walkowiak,  
Institute of Non-Ferrous Metals,  
Poland

### Reviewed by:

Xiangyu Zhao,  
Nanjing Tech University, China  
Mehmet Kadri Aydinol,  
Middle East Technical  
University, Turkey  
Timothy Sean Arthur,  
Toyota (United States),  
United States

### \*Correspondence:

Kondo-Francois Aguey-Zinsou  
f.aguey@unsw.edu.au

### Specialty section:

This article was submitted  
to Energy Storage,  
a section of the journal  
Frontiers in Energy Research

**Received:** 24 July 2017

**Accepted:** 03 October 2017

**Published:** 17 October 2017

### Citation:

Shen C and Aguey-Zinsou K-F  
(2017) Nanosized Magnesium  
Electrochemically Deposited on a  
Carbon Nanotubes Suspension:  
Synthesis and Hydrogen Storage.  
*Front. Energy Res.* 5:27.  
doi: 10.3389/fenrg.2017.00027

Herein, we report on a novel method for deposition of magnesium (Mg) nanoparticles at the surface of carbon materials. Through the suspension of carbon nanotubes (CNTs) in an electrolyte containing di-*n*-butylmagnesium as a precursor, Mg nanoparticles were effectively deposited at the surface of the CNTs as soon as these touched the working electrode. Through this process, CNTs supported Mg particles as small as 1 nm were synthesized and the distribution of the nanoparticles was found to be influenced by the concentration of the CNTs in the electrolyte. Hydrogenation of these nanoparticles at 100°C was found to lead to low temperature hydrogen release starting at 150°C, owing to shorter diffusion paths and higher hydrogen mobility in small Mg particles. However, these hydrogen properties drastically degraded as soon as the hydrogenation temperature exceeded 200°C and this may be related to the low melting temperature of ultrasmall Mg particles.

**Keywords:** electrochemical deposition, magnesium, carbon nanotubes, hydrogen storage, nanosizing

## INTRODUCTION

Magnesium (Mg) is a promising candidate for hydrogen storage with a high gravimetric capacity of 7.6 mass% H<sub>2</sub> and a volumetric density of ~110 kg m<sup>-3</sup> H<sub>2</sub> (Sun et al., 2017). However, the high stability of MgH<sub>2</sub> (75 kJ mol<sup>-1</sup> H<sub>2</sub>) induces the need of high temperatures (>300°C) to enable hydrogen release and the slow kinetics for the hydrogen sorption limit practical utilization (Lillo-Ródenas et al., 2008; Aguey-Zinsou and Ares-Fernández, 2010; Jain et al., 2010). Nanosizing is the promising approach to improve the hydrogen storage properties of Mg (Sun et al., 2017). This can be done *via* the synthesis of isolated Mg nanoparticles (Norberg et al., 2011; Shissler et al., 2014; Zou et al., 2014, 2015; Zhang et al., 2015), or their confinement in a porous host material to facilitate their stabilization (Wagemans et al., 2005; Adelmhelm and de Jongh, 2011; Zlotea et al., 2015). Carbon materials have been widely used to nanoconfine Mg and achieve better hydrogen storage properties especially in terms of kinetics (Yao et al., 2006; Lillo-Ródenas et al., 2008; de Jongh and Adelmhelm, 2010; Skripnyuk et al., 2010; Adelmhelm and de Jongh, 2011). This includes graphene, carbon nanotubes (CNTs), and carbon aerogels (Liu et al., 2013; Cai et al., 2015; Xia et al., 2015; Shinde et al., 2017). It is expected that upon particle size reduction, hydrogen kinetics will be improved owing to the shorted diffusion paths and enhanced hydrogen mobility (Corey et al., 2008; Au et al., 2014; Zlotea et al., 2015). For example, Zlotea et al. synthesized ultra-small Mg particles of 1.3 nm confined in ordered microporous carbon which started to release hydrogen below 100°C with a peak at 200°C (Zlotea et al., 2015). Nanoconfinement of Mg may

also result in improved thermodynamic properties for ultrasmall particles (<2 nm) according to theoretical calculations (Cheung et al., 2005; Wagemans et al., 2005). However, experimentally, little improvement has been observed owing to an enthalpy/entropy compensation effect (Zhao-Karger et al., 2010; Sun et al., 2017). In this context, the main improvements achieved so far through nanoconfinement have been in terms of hydrogen kinetics. The carbon scaffold is also expected to limit the growth of the Mg nanoparticles upon hydrogen cycling and, thus, lead to stable hydrogen kinetics (Zlotea et al., 2013).

Currently, Mg nanoconfinement with carbon materials is usually done *via* melt infiltration or thermal decomposition of an Mg precursor initially impregnated in the porosity of the carbon scaffold (Konarova et al., 2012; Liu et al., 2014). However, *via* these approaches control over the particle size of the nanoconfined material is often difficult because it relies on the synthesis of ordered mesoporous scaffolds. These scaffolds are also difficult to fully impregnate and the exact location of the Mg nanoparticles is hard to control.

Herein, we investigated an alternative electrochemical deposition method whereby an Mg precursor is directly reduced at the surface of carbon particles in suspension in the electrolyte. Since carbon is conductive, it is expected that every time a carbon particle touches the working electrode, the Mg precursor will be reduced at its surface and supported Mg particles will further grow. Through the functionalization of carbon particles, such an approach should not only enable control over particle size but also the location of the deposited particles. By further adjusting the deposition current, particles of different sizes can also be grown (Reetz et al., 2001). The present study reports on the potential of the approach through the electrochemical reduction of di-*n*-butylmagnesium at the surface of CNTs suspended in tetrahydrofuran (THF). CNTs were chosen as support for Mg as they can be readily dispersed in THF and have good electrical conductivity (Wang et al., 2001) to enable electron transfer between the reduced MgBu<sub>2</sub> and the electrode surface. The physical and hydrogen sorption properties of Mg nanoparticles confined/supported on these CNTs are reported and the potential of such a novel route to prepare Mg/carbon composite materials for hydrogen storage is discussed.

## MATERIALS AND METHODS

All operations were carried out under an inert atmosphere in an argon-filled LC-Technology glove box (< 1 ppm O<sub>2</sub> and H<sub>2</sub>O).

### Materials

Magnesium ribbon, platinum mesh, and platinum wire were purchased from Goodfellow, THF was purchased as HPLC grade from Fisher Scientific and dried using a LC Technology SP-1 solvent purification system. Di-*n*-butylmagnesium (MgBu<sub>2</sub>) in heptane and CNTs were from Sigma-Aldrich. Prior use, the CNTs were heat treated at 1,000°C for 2 h under a hydrogen flow of 15 ml min<sup>-1</sup> to remove any impurities and reduce most hydroxyl surface groups. After cooling, the heat treated CNTs were directly transferred and stored under high purity argon in a glove box.

## Electrochemical Synthesis of the Mg/CNTs Composite

In a typical experiment, 20 mM MgBu<sub>2</sub> was mixed with 1 mg ml<sup>-1</sup> CNTs in 18 ml THF to form the electrolyte. A 0.5 mA cm<sup>-2</sup> current was applied to reduce MgBu<sub>2</sub> at the CNTs on the Pt mesh (2 cm<sup>2</sup>) working electrode. An Mg ribbon was used as a counter electrode and a platinum wire as the reference electrode. The electrolysis proceeded for 20 h and was stopped after reaching 20 mA h to generate 9 mg of Mg and, thus, a theoretical Mg/CNTs ratio of 1:2. The concentration of CNTs was also changed to 2, 5, and 10 mg ml<sup>-1</sup> to investigate the effect of the carbon concentration in leading to a more homogeneous deposition of Mg at the CNTs surface. At the end of the electrosynthesis process, the composites were centrifuged and washed with THF then dried under vacuum to remove the residual solvent. Contrary to bare Mg nanoparticles, Mg nanoparticles supported on CNTs were not found to be flammable when exposed to air.

## Characterization of the Materials

The size, morphology, and selected area electron diffraction (SAED) were performed by transmission electron microscopy (TEM) using a Philips CM200 operated at 200 kV. For TEM analysis, the materials were grinded and dispersed in THF, sonicated for a few seconds, and then dropped onto a carbon-coated copper grid. The grid was taken in a vial filled with argon to the microscope and exposed to air during transfer to the microscope.

Structural characterization was performed by X-ray diffraction (XRD) using a Philips X'pert Multipurpose XRD system operated at 40 mA and 45 kV with a monochromated Cu K $\alpha$  radiation ( $\lambda = 1.541 \text{ \AA}$ ). Step sizes of 0.01, 0.02, or 0.05, time per step of 10 or 20 s step<sup>-1</sup> were used. The materials were protected against oxidation from air by a Kapton foil. Investigations on thermal stability by thermal gravimetric analysis (TGA), differential scanning calorimetry (DSC), and mass spectrometry (MS) analysis were performed with a Mettler Toledo TGA/DSC-1 instrument installed in a glove box filled with high purity argon (<1 ppm O<sub>2</sub> and H<sub>2</sub>O) and coupled with an OmniStar mass spectrometer (Pfeiffer). Typically, 4 mg of material was used and the analysis was run with a heating rate of 10°C min<sup>-1</sup> under a flow of argon of 25 ml min<sup>-1</sup>.

Hydrogen desorption kinetics were characterized using a high pressure magnetic balance of 1  $\mu$ g resolution equipped with capability for simultaneous density measurements (Rubotherm) (Broom, 2011). Around 30 mg of material was used and a hydrogen pressure of 3 MPa for absorption and 0.01 MPa for desorption. Hydrogen uptake and release were determined from the weight changes. For an accurate determination of the amount of hydrogen stored, a blank measurement with the empty sample holder was performed to determine the mass and volume of the sample holder. Further measurements were performed under a helium atmosphere with the material fully desorbed to determine the density of the materials and corresponding parameters for buoyancy corrections. The hydrogen absorption and desorption were performed at 300°C with 3 MPa and 0.01 MPa hydrogen pressure, respectively.

The content of Mg in the as-synthesized materials was determined by Inductively Coupled Plasma Optical Emission Spectrometry (ICP-OES) with a Perkin Elmer OPTIMA 7300 ICP-OES Instrument. Prior to analysis, the materials (~20 mg) were dissolved into 0.5 ml of concentrated nitric acid and diluted 20 times with high purity water.

## RESULTS AND DISCUSSION

We previously reported on the electrochemistry of  $\text{MgBu}_2$  and at a current of  $0.5 \text{ mA cm}^{-2}$ , this Mg precursor is readily reduced into metallic Mg (Shen and Aguey-Zinsou, 2016). The XRD pattern of the pristine CNTs (**Figure 1A**) shows the (002) peak around  $26^\circ$  corresponding to the inter-planar spacing of 0.34 nm (Kawasaki et al., 2005). However, the as-prepared Mg/CNTs composites showed in addition to the diffraction peaks of the CNTs, peaks related to the typical hexagonal Mg phase (**Figure 1A**). Furthermore, with increasing amounts of CNTs in the electrolyte, the diffraction peaks related to hexagonal Mg were found to significantly decrease in intensity and become broader; and this was interpreted in first instance as a reduction of Mg crystallite size. For the same amount of Mg electrochemically reduced, elemental analysis confirmed that the amount of Mg deposited on the CNTs is decreasing with increasing amounts of CNTs in the electrolyte

(**Figure 1B**), and this was considered as an indirect proof that Mg was effectively deposited on CNTs. This also showed that even at high amount of CNTs in the electrolyte, the reduction of  $\text{MgBu}_2$  still occurred. The evolution of the amount of Mg on CNTs also followed theoretical trends with a gap attributed to the fact that (in addition to the CNTs) some Mg is also directly deposited on the Pt working electrode.

Transmission electron microscopy analysis revealed that Mg nanoparticles (~1 nm) were effectively deposited at the surface of the CNTs. As compared to the pristine CNTs (**Figures 2A,B**), darker particles were observed after Mg deposition and this was confirmed by dark field analysis (**Figures 2C–G**). SAED analysis also corroborated the crystalline nature of the nanoparticles observed at the CNTs surface with diffraction planes corresponding to that of hexagonal Mg (**Figure 2H**). With higher amounts of CNTs in the electrolyte, the overall coverage of individual carbon tubes with Mg was also found to decrease (**Figures 2I–L**).

Considering the small particle size of the Mg observed at the CNTs surface, no diffraction peaks related to hexagonal Mg should be expected by XRD owing to the lack of long-range order of such small particles. However, the presence of Mg diffractions peaks with a crystallite size of  $\sim 26 \pm 2 \text{ nm}$  (as determined from the Scherrer equation) indicates that larger Mg particles are also contained within the material. Indeed, in addition to small Mg particles deposited at the surface of the CNTs, larger Mg particles with a size ranging from 20 to 100 nm were also observed by TEM (**Figure 2E**), in particular at low CNTs concentrations. Accordingly, the diffraction peaks observed by XRD were assigned to large Mg particles contained within the CNTs decorated with ultra-small Mg. This, thus, indicates that amounts of CNTs  $>5 \text{ mg ml}^{-1}$  should be used to achieve a better homogeneity of the material with the majority of Mg deposited at the CNTs surface.

The hydrogen sorption properties of the Mg/CNTs composite materials were also investigated and, as an example, only the behavior of the composite material synthesized with  $2 \text{ mg ml}^{-1}$  of CNTs, i.e., containing both populations of Mg at the CNTs surface and “free” larger Mg particles is reported here. As shown by XRD analysis of the materials hydrogenated at different temperatures,  $300^\circ\text{C}$  was not sufficient to achieve the full hydrogenation of the large Mg particles (**Figure 3**). At  $100^\circ\text{C}$ , no  $\text{MgH}_2$  phase appeared by XRD. However, verification of any hydrogen uptake by MS revealed that the material effectively absorbed hydrogen. Hence, as shown in **Figure 4**, hydrogen was released by the hydrogenated material from  $150^\circ\text{C}$  with a broad peak followed by significant hydrogen release peaking at  $334^\circ\text{C}$ . The low temperature hydrogen release—akin to the observations of Zlotea et al. on ultra-small Mg particles confined within an ordered mesoporous carbon (Zlotea et al., 2015)—was assigned to the ultra-small Mg particles at the CNTs surface and related to the shorted hydrogen diffusion paths and higher hydrogen mobility observed in nanosized Mg [9]. By contrast, the desorption of hydrogen observed above  $250^\circ\text{C}$  was attributed to the larger Mg particles contained within the composite material. It is noteworthy that as the temperature for hydrogenation was increased to 200 and then  $300^\circ\text{C}$ , the low-temperature hydrogen desorption

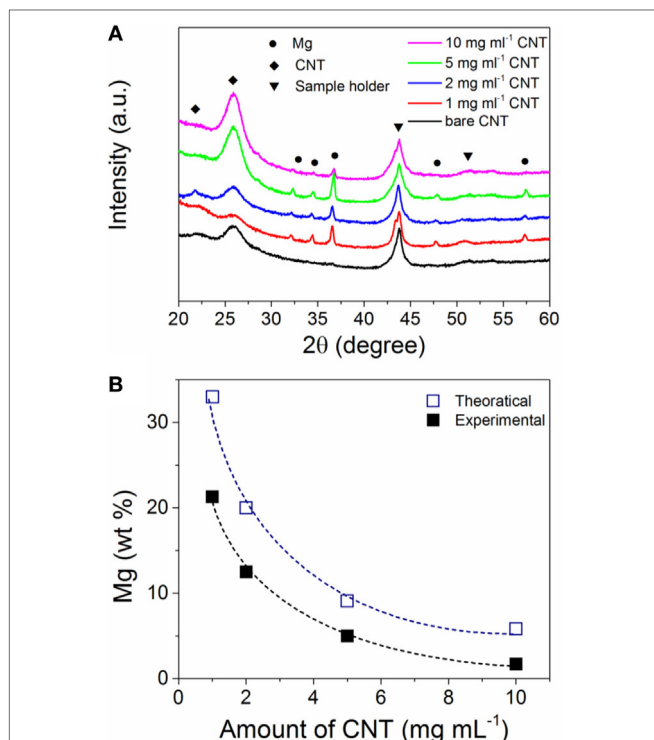


**FIGURE 1** | (A) X-ray diffraction (XRD) patterns of bare carbon nanotubes (CNTs) and electrochemically magnesium (Mg) deposited on CNTs with different amounts in the electrolyte; (B) amount of magnesium (Mg) in the Mg/CNTs composites as function of the amount of CNTs in the electrolyte. The theoretical amount of Mg deposited was calculated from the Faraday's law by considering a 2-electron reduction process.

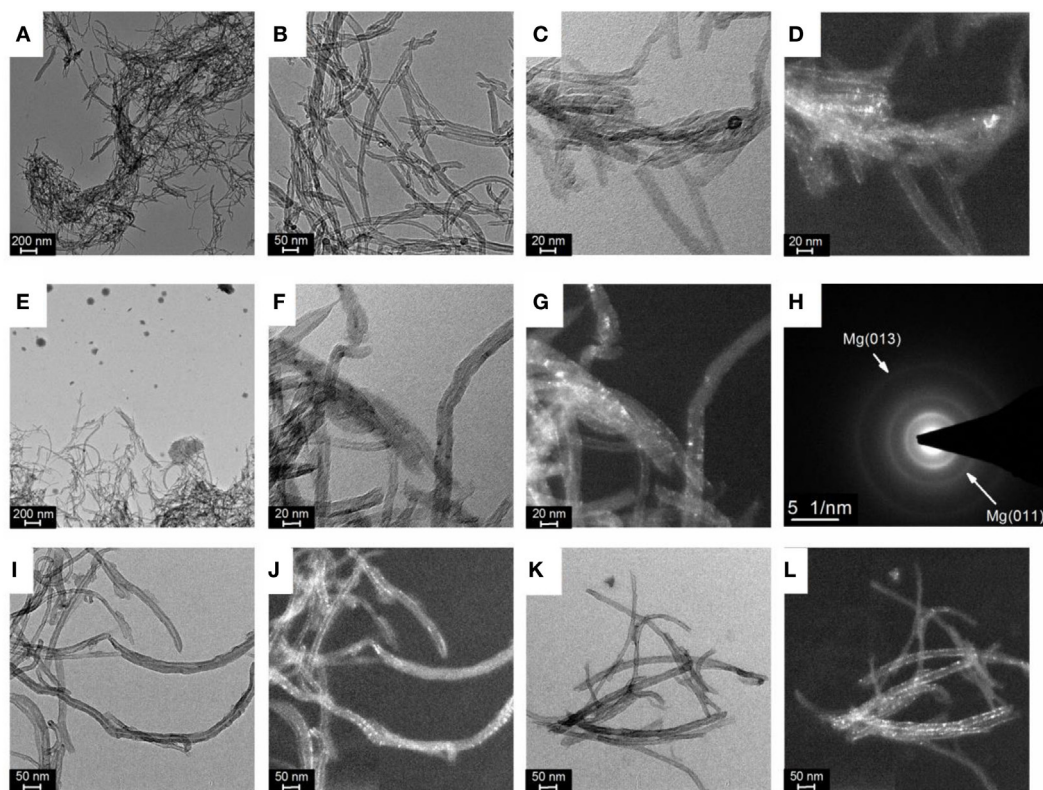


**FIGURE 2** | (A,B) Bright field of transmission electron microscopy (TEM) images of pristine carbon nanotubes (CNTs), (C) Bright field and (D) dark field TEM image of magnesium (Mg) deposited at CNTs with a concentration of  $1 \text{ mg ml}^{-1}$ , (E,F) Bright field and (G) dark field TEM image of Mg deposited at CNTs with a concentration of  $2 \text{ mg ml}^{-1}$ , (H) associated selected area electron diffraction (SAED) pattern of a dispersion of CNTs; (I) Bright field and (J) dark field TEM image of Mg deposited at CNTs with a concentration of  $5 \text{ mg ml}^{-1}$ ; (K) Bright field and (L) dark field TEM image of Mg deposited at CNTs with a concentration of  $10 \text{ mg ml}^{-1}$ .

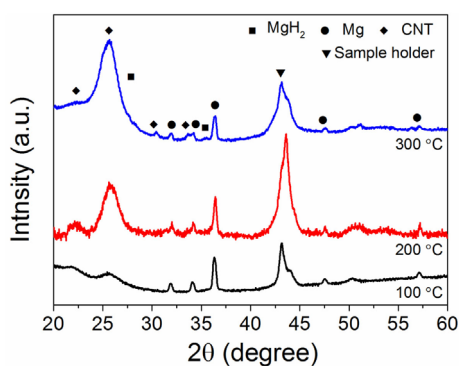


**FIGURE 3** | X-ray diffraction (XRD) of the magnesium (Mg)/carbon nanotubes (CNTs) composite (CNTs was  $2 \text{ mg ml}^{-1}$ ) as function of the hydrogenation temperature.

profile disappeared in favor of a single hydrogen desorption peak shifted at  $405^\circ\text{C}$ ; and this indicated that the CNTs supported Mg nanoparticles were extremely sensitive to temperature and their hydrogen properties degraded with increasing temperatures. One possible hypothesis is the reaction of the ultra-small Mg particles with the carbon support. However, additional SAED analysis of the material after hydrogen cycling did not reveal any

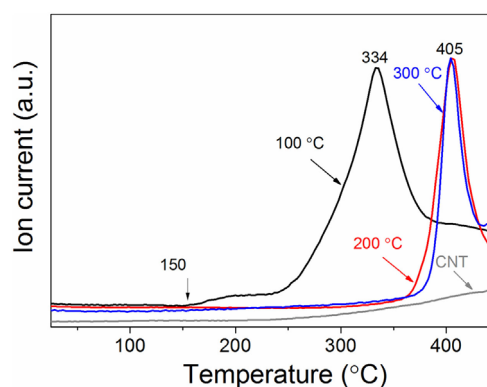


**FIGURE 4** | Hydrogen desorption profile of the magnesium/carbon nanotubes (CNTs) composite (CNTs was  $2 \text{ mg ml}^{-1}$ ) as function of the hydrogenation temperature. A heating rate of  $10^\circ\text{C min}^{-1}$  was used.

Mg carbide phase or oxide phase other than the Mg hexagonal phase (Figure 5). Previous investigations have suggested some migration/agglomeration and recrystallization of nanosized Mg confined with carbon scaffold (Zlotea et al., 2013). However, this was not clearly visible from TEM analysis (Figure 5). Mg has a melting point of  $650^\circ\text{C}$  and it can be expected that this melting

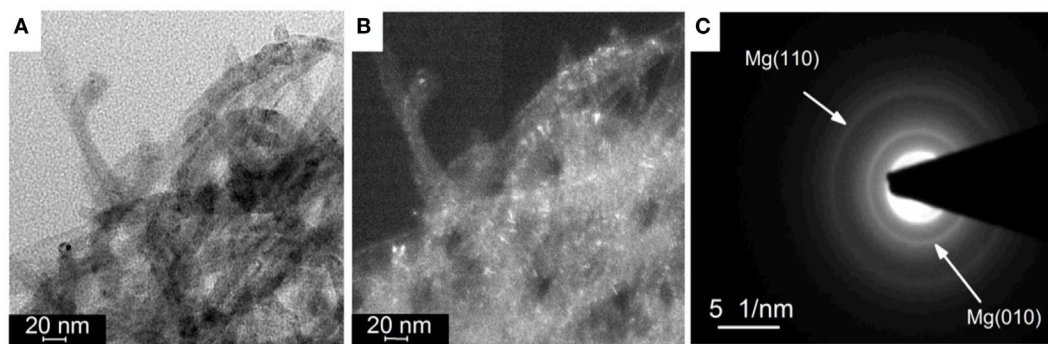


**FIGURE 5 |** (A) Bright field and (B) dark field transmission electron microscopy (TEM) image of magnesium (Mg) deposited at carbon nanotubes (CNTs) with a concentration of 2 mg ml<sup>-1</sup> after hydrogen cycling at 300°C; and (C) associated selected area electron diffraction (SAED) pattern of a dispersion of CNTs.

point will significantly decrease upon particle size reduction although this has never been reported for Mg. Nanosized Al (~ 2 nm) has been reported to have a reduced melting temperature of 200°C instead of the 660°C of the bulk material (Puri and Yang, 2007; Sun and Simon, 2007). Bulk Mg having a similar melting temperature, a reduction in melting temperature of the same order could be expected for the ultra-small Mg particles observed here. Hence, at 200°C and above significant melting of the Mg nanoparticles and potential diffusion within the carbon layers may lead to a deterioration of the hydrogen properties. Accordingly, our attempt to cycle this composite material and determine the kinetics for hydrogen uptake and release at low temperatures (<200°C) was unsuccessful. Only, a clear hydrogen release was observed at 300°C but this was attributed to the large Mg nanoparticles contained within the material.

## CONCLUSION

Magnesium–CNTs composites were successfully synthesized through electrochemical deposition with the CNTs suspended in the electrolyte, and this demonstrated for the first time an alternative method to effectively generate ultra-small Mg particles at the surface of carbon materials. Upon hydrogen absorption at 100°C hydrogenation, the composite material was found to release hydrogen from 150°C with a broad peak followed by additional hydrogen release peaking at 334°C. The hydrogen release at low temperatures was assigned to the ultra-small Mg particles on CNTs' surface, while the high temperature hydrogen desorption most likely corresponded to larger Mg particles contained within the composite material. In addition, the hydrogen

storage properties of the Mg nanoparticles supported on the CNTs was found to be extremely sensitive to temperature, with a shift of hydrogen desorption to higher temperatures as soon as the material was taken to 200°C. Such a drastic loss of low-temperature hydrogen properties was assigned to the melting of the Mg nanoparticles and the potential diffusion of Mg within the carbon layers. It is, thus, apparent that the strategy of nano-sizing Mg to enable low hydrogen cycling properties not only depends upon the ability to stabilize Mg nanoparticles but also to impede excessive reaction with the support in particular during the exothermic process of hydrogen absorption. However, assuming further functionalization of the carbon support to grow nanoparticles at specific equidistant sites, and some porosity to effectively “lock” the nanoparticle in place and restrict atomic surface diffusion of Mg, the current approach could lead to an effective way to prepare low temperature Mg-based hydrogen storage materials.

## AUTHOR CONTRIBUTIONS

Both authors contributed equally.

## ACKNOWLEDGMENTS

Financial support by UNSW Internal Research Grant program is gratefully acknowledged. We appreciate the use of instruments in the Mark Wainwright Analytical Centre at UNSW as well as equipment funded by the Australian Research Council (ARC) – Linkage, Infrastructure, Equipment and Facilities (LIEF).

## REFERENCES

- Adelhelm, P., and de Jongh, P. E. (2011). The impact of carbon materials on the hydrogen storage properties of light metal hydrides. *J. Mater. Chem.* 21, 2417–2427. doi:10.1039/c0jm02593c
- Aguey-Zinsou, K.-F., and Ares-Fernández, J.-R. (2010). Hydrogen in magnesium: new perspectives toward functional stores. *Energy Environ. Sci.* 3, 526–543. doi:10.1039/b921645f
- Au, Y. S., Obbink, M. K., Srinivasan, S., Magusin, P. C. M. M., de Jong, K. P., and de Jongh, P. E. (2014). The size dependence of hydrogen mobility and sorption kinetics for carbon-supported MgH<sub>2</sub> particles. *Adv. Funct. Mater.* 24, 3604–3611. doi:10.1002/adfm.201304060
- Broom, D. P. (2011). *Hydrogen Storage Materials. The Characterisation of Their Storage Properties*. London: Springer-Verlag.
- Cai, W., Zhou, X., Xia, L., Jiang, K., Peng, S., Long, X., et al. (2015). Positive and negative effects of carbon nanotubes on the hydrogen sorption kinetics of magnesium. *J. Phys. Chem. C* 119, 25282–25290. doi:10.1021/acs.jpcc.5b08740
- Cheung, S., Deng, W. Q., van Duin, A. C., and Goddard, W. A. III (2005). ReaxFF<sub>MgH</sub> reactive force field for magnesium hydride systems. *J. Phys. Chem. A* 109, 851–859. doi:10.1021/jp0460184

- Corey, R. L., Ivancic, T. M., Shane, D. T., Carl, E. A., Bowman, R. C., Bellosta von Colbe, J. M., et al. (2008). Hydrogen motion in magnesium hydride by NMR. *J. Phys. Chem. C* 112, 19784–19790. doi:10.1021/jp807900r
- de Jongh, P. E., and Adelhelm, P. (2010). Nanosizing and nanoconfinement: new strategies towards meeting hydrogen storage goals. *ChemSusChem* 3, 1332–1348. doi:10.1002/cssc.201000248
- Jain, I. P., Lal, C., and Jain, A. (2010). Hydrogen storage in Mg: a most promising material. *Int. J Hydrogen Energy* 35, 5133–5144. doi:10.1016/j.ijhydene.2009.08.088
- Kawasaki, S., Matsuoka, Y., Yokomae, T., Nojima, Y., Okino, F., Touhara, H., et al. (2005). XRD and TEM study of high pressure treated single-walled carbon nanotubes and C60-peapods. *Carbon N. Y.* 43, 37–45. doi:10.1016/j.carbon.2004.08.018
- Konarova, M., Tanksale, A., Beltramini, J. N., and Lu, G. Q. (2012). Porous MgH<sub>2</sub>/C composite with fast hydrogen storage kinetics. *Int. J Hydrogen Energy* 37, 8370–8378. doi:10.1016/j.ijhydene.2012.02.073
- Lillo-Ródenas, M. A., Guo, Z. X., Aguey-Zinsou, K. F., Cazorla-Amorós, D., and Linares-Solano, A. (2008). Effects of different carbon materials on MgH<sub>2</sub> decomposition. *Carbon N. Y.* 46, 126–137. doi:10.1016/j.carbon.2007.10.033
- Liu, G., Wang, Y., Jiao, L., and Yuan, H. (2014). Understanding the role of few-layer graphene nanosheets in enhancing the hydrogen sorption kinetics of magnesium hydride. *ACS Appl Mater Interfaces* 6, 11038–11046. doi:10.1021/am502755s
- Liu, Y., Zou, J., Zeng, X., Wu, X., Tian, H., Ding, W., et al. (2013). Study on hydrogen storage properties of Mg nanoparticles confined in carbon aerogels. *Int. J. Hydrogen Energy* 38, 5302–5308. doi:10.1016/j.ijhydene.2013.02.012
- Norberg, N. S., Arthur, T. S., Fredrick, S. J., and Prieto, A. L. (2011). Size-dependent hydrogen storage properties of Mg nanocrystals prepared from solution. *J. Am. Chem. Soc.* 133, 10679–10681. doi:10.1021/ja201791y
- Puri, P., and Yang, V. (2007). Effect of particle size on melting of aluminum at nano scales. *J. Phys. Chem. C* 111, 11776–11783. doi:10.1021/jp0724774
- Reetz, M. T., Winter, M., Breinbauer, R., Thurn-Albrecht, T., and Vogel, W. (2001). Size-selective electrochemical preparation of surfactant-stabilized Pd-, Ni- and Pt/Pd colloids. *Chem. Eur. J* 7, 1084–1094. doi:10.1002/1521-3765(20010302)7:5
- Shen, C., and Aguey-Zinsou, K.-F. (2016). Electrodeposited magnesium nanoparticles linking particle size to activation energy. *Energies* 9, 1073. doi:10.3390/en9121073
- Shinde, S. S., Kim, D. H., Yu, J. Y., and Lee, J. H. (2017). Self-assembled air-stable magnesium hydride embedded in 3-D activated carbon for reversible hydrogen storage. *Nanoscale* 9, 7094–7103. doi:10.1039/c7nr01699a
- Shissler, D. J., Fredrick, S. J., Braun, M. B., and Prieto, A. L. (2014). “Magnesium and doped magnesium nanostructured materials for hydrogen storage,” in *Low-Cost Nanomaterials: toward Greener and More Efficient Energy Applications*, eds Z. Lin and J. Wang New York: Springer, 297–319.
- Skripnyuk, V. M., Rabkin, E., Bendersky, L. A., Magrez, A., Carreño-Morelli, E., and Estrin, Y. (2010). Hydrogen storage properties of as-synthesized and severely deformed magnesium – multiwall carbon nanotubes composite. *Int. J Hydrogen Energy* 35, 5471–5478. doi:10.1016/j.ijhydene.2010.03.047
- Sun, J., and Simon, S. L. (2007). The melting behavior of aluminum nanoparticles. *Thermochim. Acta* 463, 32–40. doi:10.1016/j.tca.2007.07.007
- Sun, Y., Shen, C., Lai, Q., Liu, W., Wang, D.-W., and Aguey-Zinsou, K.-F. (2017). Tailoring magnesium based materials for hydrogen storage through synthesis: current state of the art. *Energy Storage Mater.* doi:10.1016/j.ensm.2017.01.010
- Wagemans, R. W., van Lenthe, J. H., de Jongh, P. E., van Dillen, A. J., and de Jong, K. P. (2005). Hydrogen storage in magnesium clusters: quantum chemical study. *J. Am. Chem. Soc.* 127, 16675–16680. doi:10.1021/ja054569h
- Wang, X. B., Liu, Y. Q., Yu, G., Xu, C. Y., Zhang, J. B., and Zhu, D. B. (2001). Anisotropic electrical transport properties of aligned carbon nanotube films. *J. Phys. Chem. B* 105, 9422–9425. doi:10.1021/jp011538
- Xia, G., Tan, Y., Chen, X., Sun, D., Guo, Z., Liu, H., et al. (2015). Monodisperse magnesium hydride nanoparticles uniformly self-assembled on graphene. *Adv. Mater.* 27, 5981–5988. doi:10.1002/adma.201502005
- Yao, X., Wu, C., Du, A., Lu, G. Q., Cheng, H., Smith, S. C., et al. (2006). Mg-based nanocomposites with high capacity and fast kinetics for hydrogen storage. *J. Phys. Chem. C* 110, 11697–11703. doi:10.1021/jp057526w
- Zhang, J., Yu, X. F., Mao, C., Long, C. G., Chen, J., and Zhou, D. W. (2015). Influences and mechanisms of graphene-doping on dehydrogenation properties of MgH<sub>2</sub>: experimental and first-principles studies. *Energy* 89, 957–964. doi:10.1016/j.energy.2015.06.037
- Zhao-Karger, Z., Hu, J., Roth, A., Wang, D., Kubel, C., Lohstroh, W., et al. (2010). Altered thermodynamic and kinetic properties of MgH<sub>2</sub> infiltrated in microporous scaffold. *Chem. Commun.* 46, 8353–8355. doi:10.1039/C0CC03072D
- Zlotea, C., Cuevas, F., Andrieux, J., Matei Ghimbeu, C., Leroy, E., Léonel, E., et al. (2013). Tunable synthesis of (Mg–Ni)-based hydrides nanoconfined in templated carbon studied by in situ synchrotron diffraction. *Nano Energy* 2, 12–20. doi:10.1016/j.nanoen.2012.07.005
- Zlotea, C., Oumellal, Y., Hwang, S. J., Ghimbeu, C. M., De Jongh, P. E., and Latroche, M. (2015). Ultrasmall MgH<sub>2</sub> nanoparticles embedded in an ordered microporous carbon exhibiting rapid hydrogen sorption kinetics. *J. Phys. Chem. C* 119, 18091–18098. doi:10.1021/acs.jpcc.5b05754
- Zou, J. X., Long, S., Chen, X., Zeng, X. Q., and Ding, W. J. (2015). Preparation and hydrogen sorption properties of a Ni decorated Mg based Mg@Ni nanocomposite. *Int. J Hydrogen Energy* 40, 1820–1828. doi:10.1016/j.ijhydene.2014.11.113
- Zou, J. X., Long, S., Zhang, L. F., Lu, C., Chen, X., Zeng, X. Q., et al. (2014). Hydrogen sorption behaviors of a core-shell structured Mg@Fe composite powder. *Mater. Trans. Jim* 55, 1156–1160. doi:10.2320/matertrans.MG201418

**Conflict of Interest Statement:** The authors declare that the research was conducted in the absence of any commercial or financial relationships that could be construed as a potential conflict of interest.

Copyright © 2017 Shen and Aguey-Zinsou. This is an open-access article distributed under the terms of the Creative Commons Attribution License (CC BY). The use, distribution or reproduction in other forums is permitted, provided the original author(s) or licensor are credited and that the original publication in this journal is cited, in accordance with accepted academic practice. No use, distribution or reproduction is permitted which does not comply with these terms.